Journal of Applied Polymer Science

Controllable Reinforcement of Stiffness and Toughness of Polypropylene via Thermally Induced Self-Assembly of β-Nucleating Agent

Yijun Li, Xinyu Wen, Min Nie, Qi Wang
State Key Laboratory of Polymer Materials Engineering, Polymer Research Institute of Sichuan University, Chengdu 610065, China
Correspondence to: M. Nie (E-mail: poly.nie@gmail.com)

ABSTRACT: An easy approach was reported to achieve the simultaneous reinforcement and toughening of polypropylene (PP) via thermally induced self-assembly of β-nucleating agent (TMB-5). The results showed that the processing temperatures dictated the solubility and self-assembly of TMB-5 in the polymer melts to determine the subsequent morphology development of PP. At low processing temperature, TMB-5 did not dissolve into the polymer melt but remained original shape to induce PP to crystallize into spherulites so that it only promoted the formation of β-form crystals to enhance the toughness of the samples. At high processing temperature, TMB-5 gradually dissolved into the polymer melts. On cooling, the dissolved nucleating agent self-assembled into high aspect ratio fibrils through intermolecular hydrogen-bonding interactions. Due to a favorable matching between PP and TMB-5, PP preferred to nucleate and grow orthogonally to the fibril axis and into oriented hybrid shish-kebab morphology with rich β-form crystals. Compared with isotropic spherulites, the anisotropic structure exhibited excellent properties of the β-form crystal and shish-kebab morphology to simultaneously improve the strength and toughness of TMB-5-modified PP samples. With the increasing processing temperature, more dissolved TMB-5 was involved in the self-assembly procedure to generate longer fibrils and induce more lamellae to grow on the surface. As a consequence, the anisotropy of the PP samples increased further, bringing out more improvements of the tensile strength. © 2014 Wiley Periodicals, Inc. J. Appl. Polym. Sci. **2014**, *131*, 40605.

KEYWORDS: self-assembly; properties and characterization; surfaces and interfaces

Received 23 December 2013; accepted 12 February 2014
DOI: 10.1002/app.40605

INTRODUCTION

The properties of semicrystalline polymer materials do not only depend on their chemical structure but also depend on the morphology and nature of the crystalline phase developing during the processing.[1,2] Thus, it is technologically important and scientifically fascinating to design and tailor hierarchical structures at different levels for the polymer products with excellent performances.[3]

Polypropylene (PP) is a typical polymorphic polymer, capable to form three kinds of modifications,[4] namely monoclinic α form, hexagonal β form, and triclinic γ form. It has been well demonstrated that the stacking of β-form crystal is relatively friable, and thus, when impact occurs, lamellar crystal easily slips with energy absorbed.[5,6] Therefore, the formation of β-form crystals is favorable to enhance the impact toughness of PP. However, β-form crystal is a metastable phase and is produced only under special processing conditions. Adding β-nucleating agent is an effective way to promote β-form crystal to solve the problem of low impact resistance. Unfortunately, when the PP product becomes tougher due to the domination of β-form crystals, it suffers tremendous decrease in strength which restricts the application of PP materials.[7] Hence, it is extremely difficult and significant to simultaneously increase toughness and strength of PP products by directly adding β-nucleating agent.[8,9]

Spherulite and shish-kebab are two mainly yielded morphologies during the process of polymers.[10] Compared with isotropic spherulites, anisotropic shish-kebab brings out outstanding strength in the orientation direction.[11–13] Although the polymer melts are subjected to the shear field at the initial stage in normal injection molding,[14] the preoriented structures easily relax back into the random state due to the thermal motions during the subsequent quiescent melt solidification. As a result, only isotropic spherulites are generated, and it is a huge challenge to obtain high amount of shish-kebab crystals with reinforcement function via normal injection molding.[15]

© 2014 Wiley Periodicals, Inc.

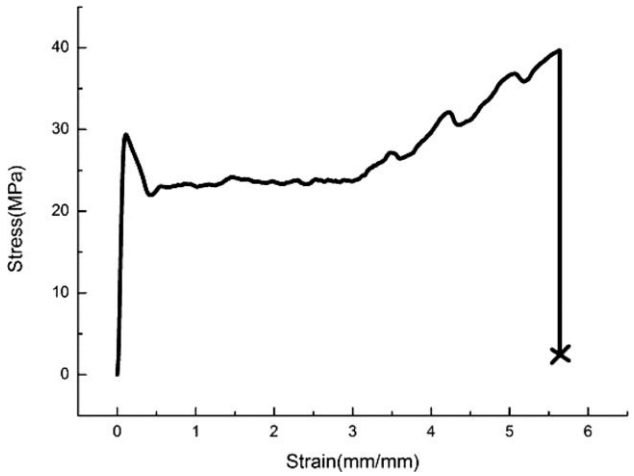

Figure 1. Typical strain–stress curve of TMB-5-modified PP samples.

Intelligent works of Li et al.[16] showed a fascinating hybrid shish-kebab morphology through interfacial crystallization, which contained the shish of anisotropic fibrous filler and the kebabs of polymer. The hybrid shish-kebab morphology can facilitate the enhancement of the performances.[17–19] Ning et al. used carbon nanotubes and whisker as a template to induce epitaxial crystallization of PP on their surfaces and form hybrid shish-kebab to substantially improve its tensile strength, hardness, and thermal stability.[20] Recently, some nucleating agents with hydrogen bonds were identified to self-assemble into diverse topological structures.[21–23] It was also reported that the self-assembled structure as a template could direct the following lateral growth of the chain-folded lamella into different morphologies.[24–27] For instance, Varga prepared PP samples with spherulite, fibrous, dendric morphology by adjusting the melting temperature and concentration of the nucleating agent.[6] Dong indicated effect of final heating temperature on dissolution of β-nucleating agent and the following supermolecular structure of PP.[28,29] Therefore, it is expected that reinforcement and toughening for PP can be achieved through regulation on self-assembly of β-nucleating agent to generate fine fibers and induce epitaxial growth of PP into hybrid shish-kebab morphology with rich β-form crystals. Surprisingly, little attention has been paid to controlling over the self-assembly of β-nucleating agent fiber to form the hybrid shish-kebab with high aspect ratio and its effect on the performances of PP.[30–32] This is because the β-nucleating agents generally are added to the PP matrix at a lower temperature ($\leq$210°C), where the nucleating agent cannot dissolve in the matrix and self-assemble into the fiber but remain original structure. As a result, only spherulites with rich β-form crystal are obtained, which cannot achieve reinforcement and toughening for PP.[33]

In this article, TMB-5, an efficient β-nucleating agent, was added into PP matrix and its self-assembly behavior was regulated to obtain the fibrils with different aspect ratios in injection-molded process. Moreover, a systematic investigation on the processing temperature, morphological development, and macroscopic properties was conducted. Eventually, the mechanism of self-assembly nucleating agent with available temperature control and the relationship between hybrid shish-kebab morphology and the performances were revealed.

EXPERIMENTAL

Material

A commercially available isotactic PP (trade name T30S), provided by Dushanzi Petroleum Chemical Incorporation (Xinjiang, China), was used in this study. Its weight average molecular weight was 39.9 $\times$ 10^4 g/mol and the molecular weight distribution (M_w/M_n) was ~4.6.

β-Nucleating agent, aryl amide-based compound TMB-5, was purchased from Shanxi Chemical Industry Research Institute (Shanxi, China).

Sample Preparation

The PP and TMB-5 powder was first melt compounded to make a master-batch containing 1 wt % TMB-5 in a corotating twin screw extruder, and then was diluted by adding pure PP and extruded to prepare PP specimens containing 0.1 wt % TMB-5. The pelletized granules were subsequently injection molded under different processing temperatures of 190, 210,

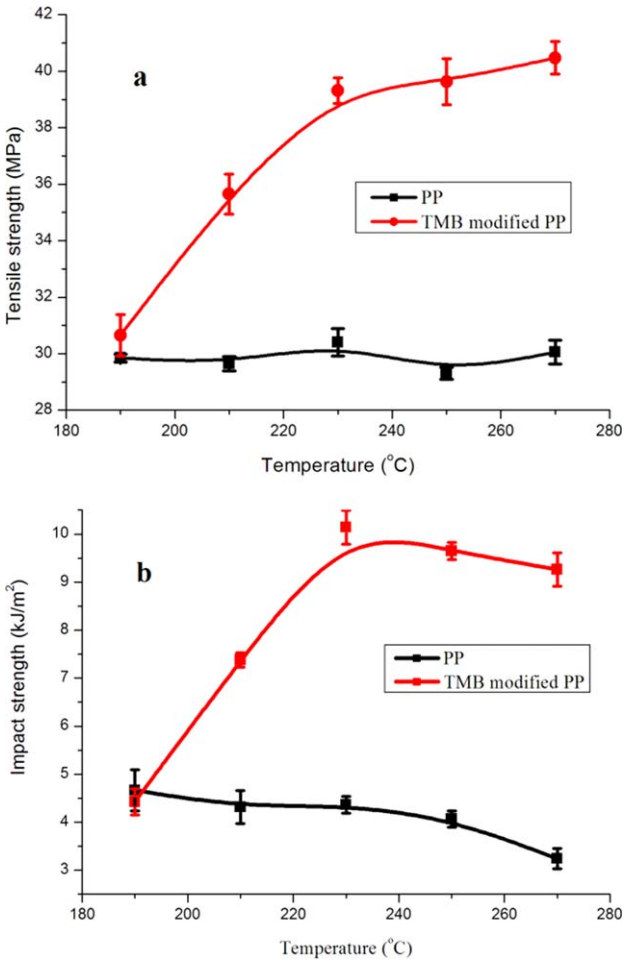

Figure 2. Effects of processing temperatures on (a) tensile strengths and (b) impact strengths of pure PP and TMB-5-modified PP samples. [Color figure can be viewed in the online issue, which is available at wileyonlinelibrary.com.]

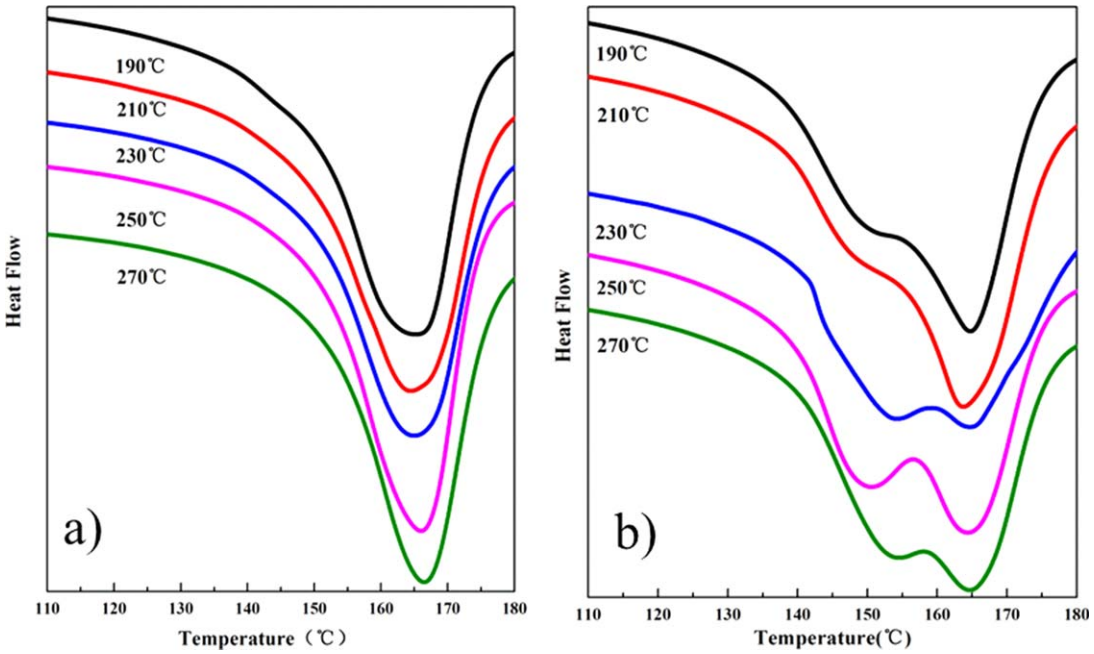

Figure 3. DSC curves for (a) pure PP and (b) TMB-5-modified PP samples prepared at different processing temperatures. [Color figure can be viewed in the online issue, which is available at wileyonlinelibrary.com.]

230, 250, and 270°C. For comparison purpose, the injection-molded samples of pure PP were also prepared under the same processing condition.

CHARACTERIZATION

Mechanical Properties

The tensile test was conducted with a universal testing machine (model RG L-10, Shenzhen Reger Instrument Co.) according to GB/T 1040-92. The tested samples were dumbbell-like bars with the dimension of 100 × 10 × 4 mm^3. The cross-head speed was 20 mm/min. A typical strain–stress curve of TMB-5-modified PP sample prepared at 230°C is shown in Figure 1. Tensile strength which was defined as the maximum stress it could be subjected to before fracture.

The notched izod impact strength of the samples with a V-notch of 2 mm depth was tested using an izod machine XBJ-7.5/11 (Chang Chun Testing Machine Co.) according to the GB/T1834-1996.

Differential Scanning Calorimetry

The thermal analysis of the samples was conducted using a Q20 differential scanning calorimetry (DSC) apparatus (TA, America), calibrated using indium and zinc standards. The 5–8 mg specimens were heated from 50 to 200°C with a heating rate of 30°C/min, under nitrogen flow.

Optical Microscopy (POM)

The crystalline morphologies of the samples at various processing temperatures were observed by polarized light microscope (Leica DM2500P) connected to a hot stage (Linkam THMS600, Linkam Scientific Instruments, UK) and a Pixelink camera (PL-A662). Moreover, TMB-5-modified PP samples also were heated to 190°C at a rate of 30°C/min to melt PP to observe topological structures of the nucleating agent.

Wide-Angle X-ray Diffraction (XRD)

The crystalline structure of the samples was investigated by a DX-1000 diffractometer (Dandong Fangyuan Instrument Co., China), in which CuK_α radiation was operated at 40 kV and 25 mA. The scanning 2θ range was 10–30° with a scanning rate of 1°/s. The relative amount of β-form crystal was calculated according to Tuner–Jones equation[34]:

Table I. Summary of the Data Obtained from DSC Curves

	Pure PP samples					TMB-5 modified PP samples				
Tem. (°C)	190	210	230	250	270	190	210	230	250	270
ΔH (J/g)	62.7	87.6	84.8	74.0	82.9	90.6	92.6	88.0	88.9	89.8
ΔH_α (J/g)	62.7	87.6	84.8	74.0	82.9	52.5	49.5	33.5	27.6	22.5
ΔH_β (J/g)	-	-	-	-	-	38.2	43.1	54.5	61.3	67.4
K_β (%)	-	-	-	-	-	42.1	46.5	61.9	68.9	75.0

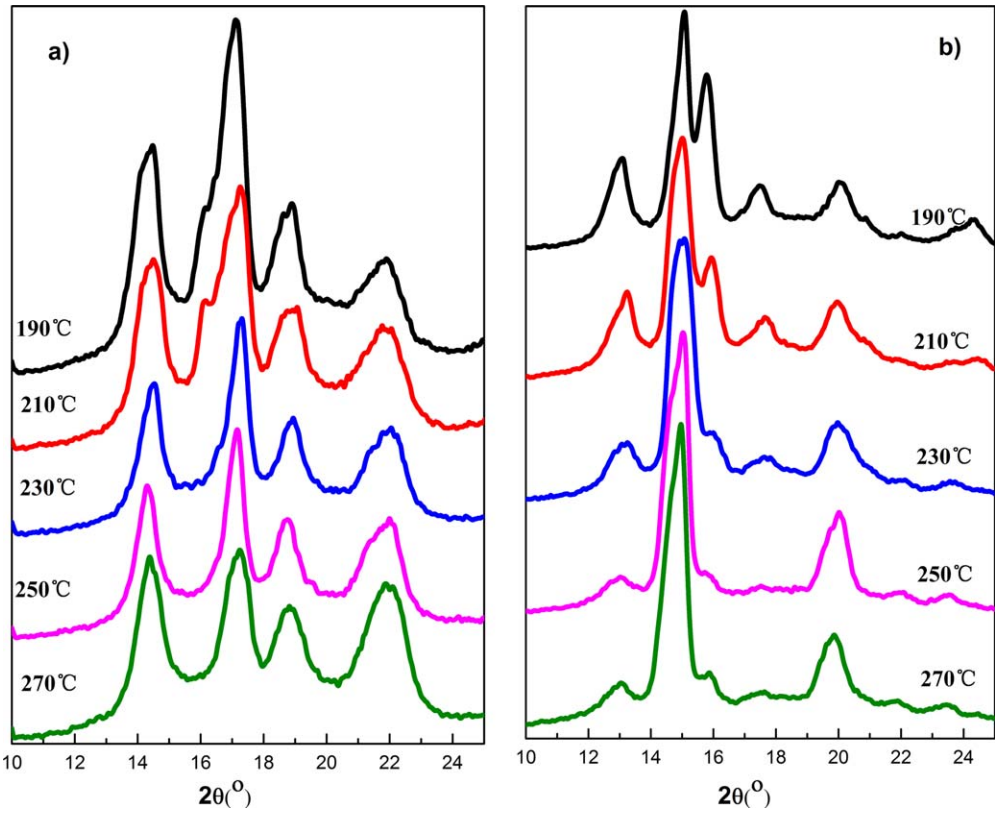

Figure 4. XRD curves for (a) pure PP and (b) TMB-5-modified PP samples prepared at different processing temperatures. [Color figure can be viewed in the online issue, which is available at wileyonlinelibrary.com.]

$$K_\beta = \frac{H_{\beta(300)}}{H_{\alpha(100)} + H_{\alpha(040)} + H_{\alpha(130)} + H_{\beta(300)}} \quad (1)$$

where $H_\beta(300)$ was the peak intensity of the $\beta(300)$ plane, and $H_\alpha(100)$, $H_\alpha(040)$, and $H_\alpha(130)$ were the peak intensity of $\alpha(110)$, $\alpha(040)$, and $\alpha(130)$ planes, respectively.

Scanning Electron Microscopy

The scanning electron microscopy (SEM) specimens were directly cut from the tensile bars and etched by permanganic etchant for 48 h at room temperature to remove the amorphous phase. Then, the etched samples were carefully cleaned by diluents sulfuric, hydrogen peroxide, and acetone, coated with gold and observed by an Inspect F(FEI) scanning electron microscopy instrument at 0.5 Torr and 20 kV.

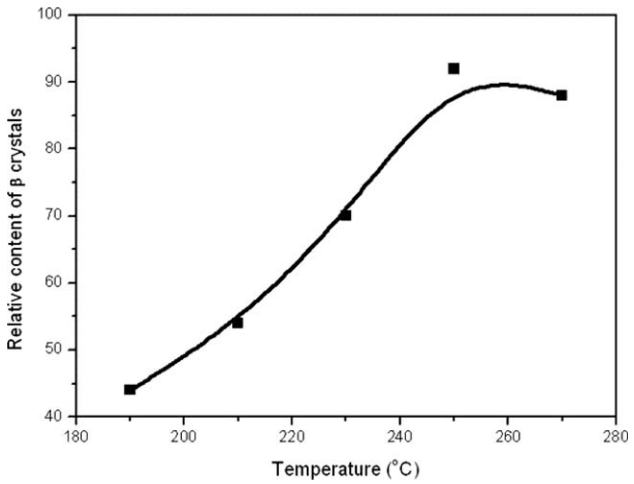

Figure 5. Effects of processing temperatures on relative contents of β crystals of TMB-5-modified PP from XRD curves.

RESULTS

Tensile strength and impact strength of pure PP and TMB-5-modified PP samples are shown in Figure 2. For pure PP samples, the processing temperature had little effect on their performances and their tensile strength and impact strength were about 30 MPa and 4.3 kJ/m^2, respectively. When small quantities of TMB-5 were added into PP matrix, the samples exhibited more excellent mechanical properties, and an inspiring increase was observed when the processing temperature exceeded a critical temperature of 210°C. Tensile strength and impact strength of TMB-5-modified PP samples prepared at 270°C reached 40.5 MPa and 9.3 kJ/m^2, respectively, increased by 35 and 186% compared to that of pure PP prepared at 270°C. This indicated that the simultaneous reinforcement and toughening of PP were successfully achieved through regulating the processing temperature.

Figure 3 shows the DSC heating scan of pure PP and TMB-5-modified PP under different processing temperatures. Pure PP only displayed a single sharp melting peak of α-form crystals at 168°C, while two melting peaks could be detected at ~167°C and 154°C in TMB-modified PP samples, which represented the

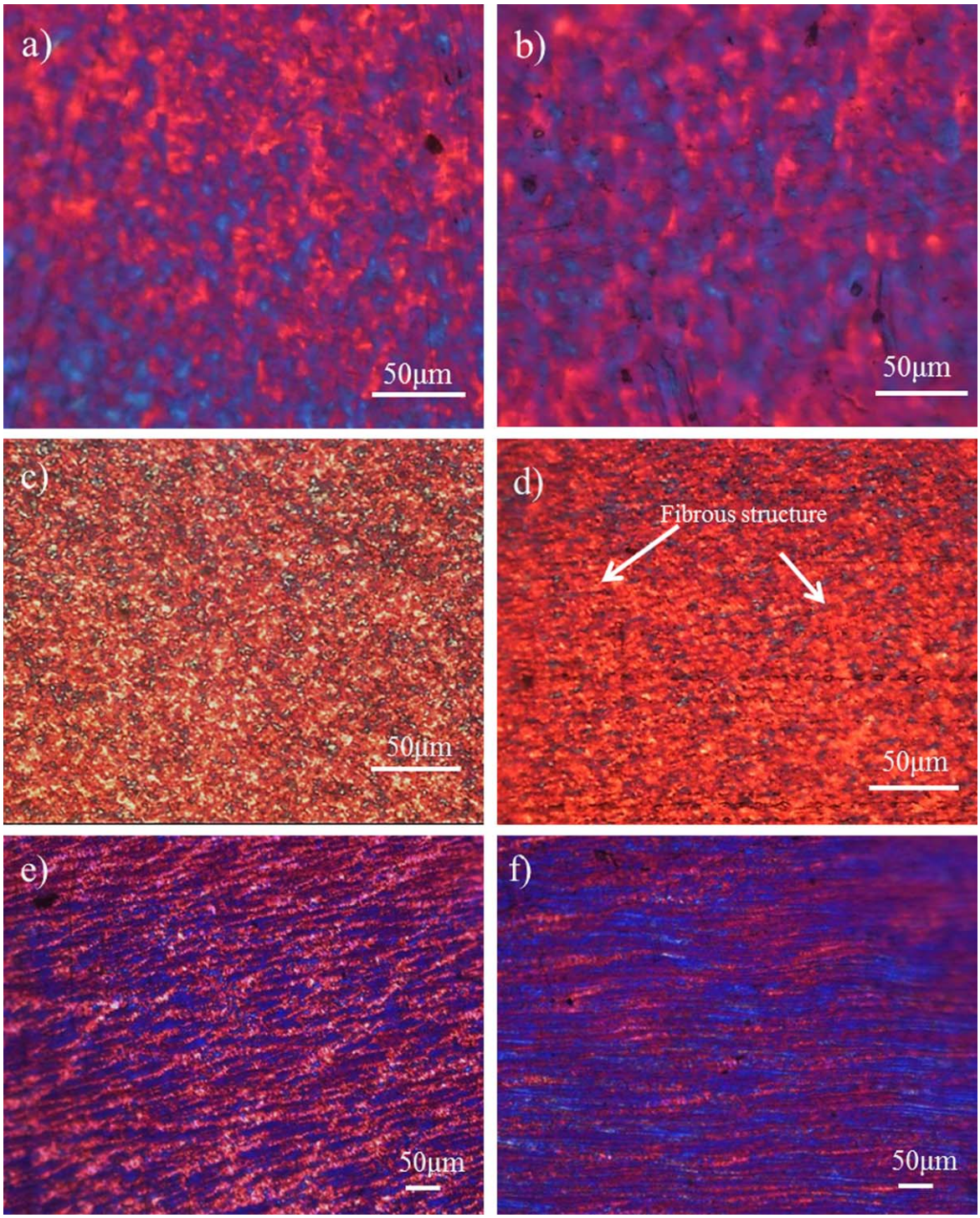

Figure 6. POM photos of pure PP samples prepared at (a) 190°C and (b) 270°C and TMB-5-modified PP samples prepared at (c) 190°C, (d) 210°C, (e) 230°C, and (f) 270°C. [Color figure can be viewed in the online issue, which is available at wileyonlinelibrary.com.]

existence of α- and β-form crystals, respectively.[35] Moreover, with the increasing processing temperatures, TMB-5-modified PP exhibited more pronounced melting peak of β-form crystals, indicating that massive β-form crystals were induced by TMB-5 at high processing temperatures. The values of enthalpy from α- and β-form crystals were obtained by peak fitting of DSC curves and the relative content of β-form crystals was equal to the fraction of the enthalpy from β-form crystals in all fusion enthalpy. The results are listed in Table I. Clearly, TMB-5 could promote the formation of β-form crystals. However, β-form crystals could transformed into α-form crystals during the heating process of DSC test, which were widely reported and

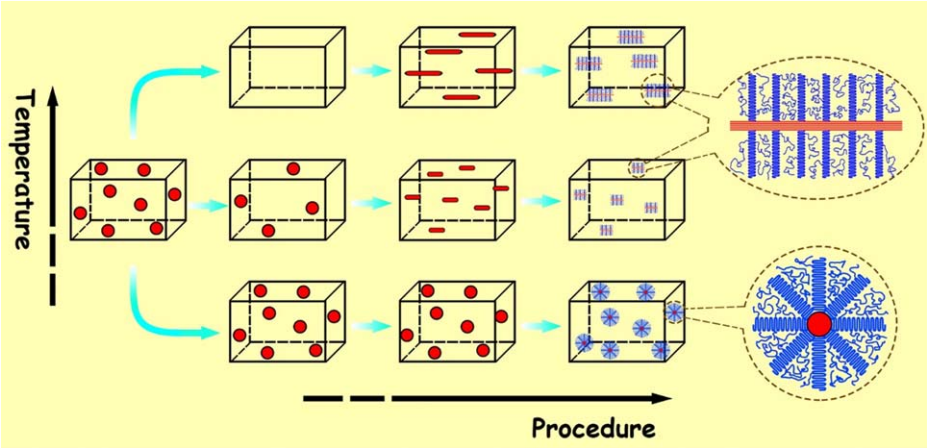

Figure 7. Schematic illustration of the relation between the dissolution and self-assembly of the nucleating agent and the subsequent morphology of PP. [Color figure can be viewed in the online issue, which is available at wileyonlinelibrary.com.]

accepted.[36] Therefore, for a more accurate estimation of the relative content of β-form crystal, XRD experiments were carried out. As shown in Figure 4, pure PP samples showed the five typical diffraction peaks at $2\theta = 13.9°$, 16.8°, 18.4°, 20.9°, and 21.6° corresponding to the (110), (040), and (130), overlapping (111), and (131) reflections of the α-form crystal, respectively. For TMB-5-modified PP samples, the characteristic peak of the (300) plane of the β-form crystals was identified at diffraction angle $2\theta = 16.0°$, which reflected a high relative content of β-form crystal. The relative content of β-form crystals in TMB-5-modified PP samples was calculated according to Tuner–Jones equation and the results are present in Figure 5. Undeniably,

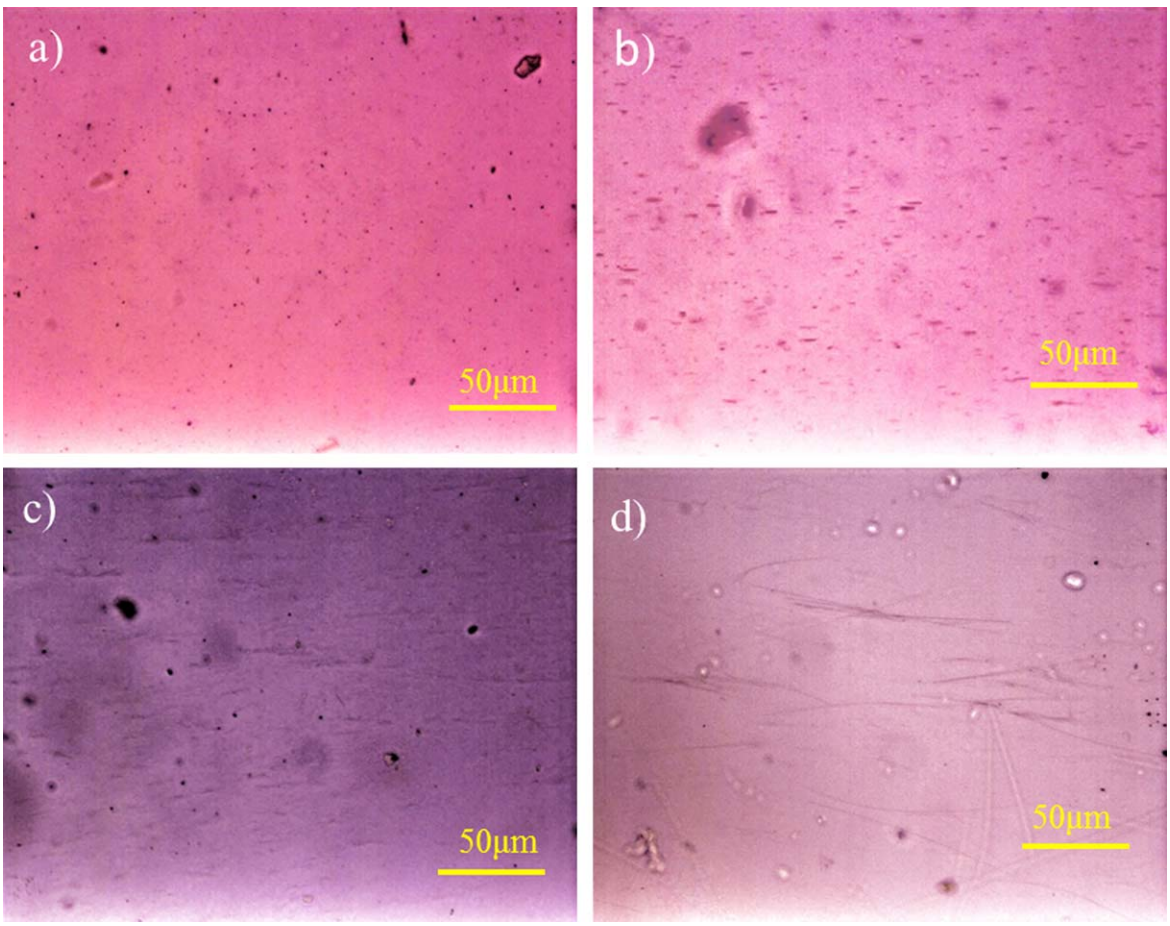

Figure 8. Topological structures of TMB-5 in PP matrix prepared at (a) 190°C, (b) 210°C, (c) 230°C, and (d) 270°C. [Color figure can be viewed in the online issue, which is available at wileyonlinelibrary.com.]

with the increasing processing temperature, more β-form crystals were generated. When the processing temperature was 250°C, the relative content of β-form crystals reached 92%. This was reasonable due to the phase transformation from β to α form during the heating process.

The morphology of the pure PP and TMB-5-modified PP samples was also investigated by POM. As the processing temperatures did not affect the morphology of pure PP samples obviously, here we presented two typical micrographs at the extreme temperatures of 190 and 270°C. As shown in Figure 6, pure PP only exhibited isotropic spherulites. With the addition of TMB-5, the morphology of PP altered dramatically. At low processing temperature of 190°C, the size of spherulites reduced compared to that in pure PP. Very wondrously, when the temperature exceeded 210°C, the morphology was transformed gradually into anisotropic fibrous crystals and with the increasing temperatures, the length of the fiberlike crystals increased.

DISCUSSION

Dependence of the morphology and modification of PP on the processing temperatures can be ascribed to the solubility of the β-nucleating agent in the polymer melts.[6,36] It is generally accepted that high temperatures can cause more TMB-5 dissolve. On the one hand, nucleation is the first step for polymer crystallization. The formation of nuclei requires the negative Gibbs free energy of the system (ΔG), which is dictated by the work required to build the new interface (ΔGs) and the energy gained due to the increased order of polymer chains (ΔGv),[37] that is, $\Delta G = \Delta Gs + \Delta Gv$. Due to a favorable matching between the crystal lattices of PP and TMB-5,[38] the surface of TMB-5 hosts a large number of nucleation sites for the epitaxial growth of PP. As a result, introduction of the nucleation sites could reduce ΔGs, and thus, activation energy for heterogeneous nucleation on the surface of the TMB-5 is lower than that for homogeneous nucleation of PP itself. Most of the polymers "prefer" to nucleate and grow on the surface of TMB-5. Because of selective nucleating effect of TMB-5 on β-form crystals, a large amount of PP crystallizes into β-form crystals, and good dissolution can promote the homogeneous dispersion of nucleating agent in the matrix so as to improve the nucleating efficiency and increase the content of β-form crystals.[39] Accordingly, TMB-5-modified PP exhibited higher impact strength compared to that of pure PP with α-form crystals, and more enhancements were achieved at higher processing temperatures.

On the other hand, the topological structure of the initial nuclei often dictates the subsequent development of morphology.[40] Pointlike nuclei from homogeneous nucleation can induce the formation of spherulites, whereas fiberlike nuclei can promote the epitaxial growth of folded-chain lamellae perpendicular to its surface, and generate anisotropic shish-kebab structure which is composed of the oriented fibril and encircled layered lamellar (kebabs). Accordingly, the presence of the preoriented precursors is a prerequisite for formation of the anisotropic morphology. Although the chains undergo a transition from a coiled conformation to a highly oriented state under flow, the preoriented structure is unstable and is readily to relax back into the random state.[22,41] Thus, there were only isotropic spherulites generated in pure PP samples. Compared to the oriented molecular chains, the nucleating agent is quite stable and the relaxation time of the inorganic compound is often longer than 2000 s.[25,42] Once recrystallized in the polymer melt, the formed structure will not be destroyed and direct the crystallization of polymer to form diverse morphologies. Figure 7 represents schematic illustration of the relation between the dissolution and self-assembly of the nucleating agent and the subsequent morphology of PP. At low processing temperature, TMB-5 could not dissolve into the polymer melt so it remained original pointlike shape to induce PP crystallize into spherulites. Hence, its tensile strength nearly was the same as that of pure PP. With the increasing processing temperature, TMB-5 gradually dissolved into the polymer melts. On cooling, the dissolved nucleating agent could self-assemble into high aspect ratio fibrils through intermolecular hydrogen-bonding interactions. Obviously, the premise to form the fibrous structure was the dissolution of nucleating agent. At high processing temperatures, more dissolved TMB-5 was involved in the self-assembly procedure to generate longer fibrils. It was proved by the

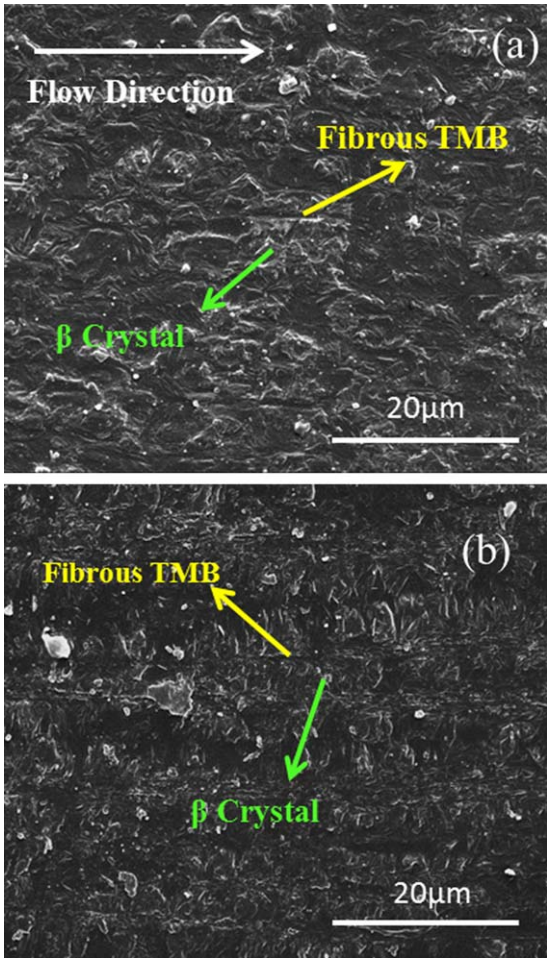

Figure 9. SEM photos of TMB-5-modified PP samples prepared at (a) 210°C and (b) 270°C. [Color figure can be viewed in the online issue, which is available at wileyonlinelibrary.com.]

topological structures of TMB-5 in PP matrix shown in Figure 8, which were obtained after heating TMB-5-modified PP samples to 190°C. At this temperature, PP melted while the nucleating agent unchanged. Subsequently, PP grew epitaxially on the surface of the fibrous nucleating agents and into an oriented hybrid shish-kebab morphology. During the injection processing, the fibrous nucleating agents preferred to align along the direction of the flow so that their alignment was transformed into the orientation of polymer lamellae with the templating mechanism. SEM photos in Figure 9 showed the refined structure of TMB-5-modified PP at the different processing temperatures. As the etchant would first remove nucleating agents, an array of groove in Figure 9(a,b) represented the location of the nucleating agents. Apparently, the structure of the nucleating agents was fibrous with their long axis parallel to the extrusion direction and the lamellae stacked on both sides of the fibrous nucleating agents. The anisotropic hybrid shish-kebab structure could improve mechanical properties dramatically in the orientation direction. With the increasing processing temperature, the fibrous nucleating agent became longer to induce more lamellae to grow on the surface. As a consequence, the anisotropy of the PP samples increased further, bringing out more improvements of the tensile strength.

CONCLUSIONS

This article successfully controlled the crystal nature and morphology of PP through regulation on self-assembly of β-nucleating agent to prepare PP with excellent performances. The results showed that depending on the processing temperature, TMB-5 could self-assemble into the fibrils. Compared to the oriented molecular chains, the nucleating agent was quite stable and served as oriented template to direct the epitaxial crystallization of polymer into hybrid shish-kebab morphology with rich β-form crystals. As a result, tremendous enhancement of mechanical properties was achieved in TMB-5-modified PP samples. The tensile strength and impact strength of TMB-5-modified PP samples reached 40.5 MPa and 9.3 kJ/m^2, respectively, 35% and 186% higher than that of pure PP samples. This study could provide a new way to achieve the simultaneous reinforcement and toughening of PP through designing and tailoring special hierarchical structure.

ACKNOWLEDGMENTS

This work is financiered by the National Natural Science Foundation of China (51127003, 51303114, and 51121001).

REFERENCES

1. Lin, Y.; Chen, H.; Chan, C.-M.; Wu, J. *J. Macromol.* **2008**, *41*, 9204.
2. Ljungberg, N.; Cavaille, J. Y.; Heux, L. *Polymer* **2006**, *47*, 6285.
3. Kimata, S.; Sakurai, T.; Nozue, Y.; Kasahara, T.; Yamaguchi, N.; Karino, T.; Shibayama, M.; Kornfield, J. A. *Science* **2007**, *316*, 1014.
4. Varga, J. *J. Macromol. Sci. Phys.* **2002**, *B41*, 1121.
5. Chu, F.; Yamaoka, T.; Kimura, Y. *Polymer* **1995**, *36*, 2523.
6. Varga, J.; Menyhard, A. *Macromolecules* **2007**, *40*, 2422.
7. Wang, Y.; Zhang, Q.; Na, B.; Du, R.; Fu, Q.; Shen, K. *Polymer* **2003**, *44*, 4261.
8. Schrauwen, B. A. G.; Breemen, L. C. A. v.; Spoelstra, A. B.; Govaert, L. E.; Peters, G. W. M.; Meijer, H. E. H. *Macromolecules* **2004**, *37*, 8618.
9. Chen, Y.-H.; Zhong, G.-J.; Wang, Y.; Li, Z.-M.; Li, L. *Macromolecules* **2009**, *42*, 4343.
10. Bai, H. W.; Xiu, H.; Gao, J.; Deng, H.; Zhang, Q.; Yang, M. B.; Fu, Q. *ACS Appl. Mater. Interfaces* **2012**, *4*, 897.
11. Yan, B. W.; Wu, H.; Jiang, G. J.; Guo, S. Y.; Huang, J. A. *ACS Appl. Mater. Interfaces* **2010**, *2*, 3023.
12. Agarwal, P. K.; Somani, R. H.; Weng, W. Q.; Mehta, A.; Yang, L.; Ran, S. F.; Liu, L. Z.; Hsiao, B. S. *Macromolecules* **2003**, *36*, 5226.
13. Yang, H. R.; Lei, J.; Li, L. B.; Fu, Q.; Li, Z. M. *Macromolecules* **2012**, *45*, 6600.
14. Somani, R. H.; Hsiao, B. S.; Nogales, A.; Srinivas, S.; Tsou, A. H.; Sics, I.; Balta-Calleja, F. J.; Ezquerra, T. A. *Macromolecules* **2000**, *33*, 9385.
15. Wang, K.; Chen, F.; Zhang, Q.; Fu, Q. *Polymer* **2008**, *49*, 4745.
16. Li, L.; Li, C. Y.; Ni, C. *J. Am. Chem. Soc.* **2006**, *128*, 1692.
17. Zhang, S. J.; Lin, W.; Wong, C. P.; Bucknall, D. G.; Kumar, S. *ACS Appl. Mater. Interfaces* **2010**, *2*, 1642.
18. Laird, E. D.; Li, C. Y. *Macromolecules* **2013**, *46*, 2877.
19. Ning, N.; Fu, S.; Zhang, W.; Chen, F.; Wang, K.; Deng, H.; Zhang, Q.; Fu, Q. *Prog. Polym. Sci.* **2012**, *37*, 1425.
20. Ning, N. Y.; Luo, F.; Wang, K.; Du, R. N.; Zhang, Q.; Chen, F.; Fu, Q. *Polymer* **2009**, *50*, 3851.
21. Luo, F.; Geng, C.; Wang, K.; Deng, H.; Chen, F.; Fu, Q.; Na, B. *Macromolecules* **2009**, *42*, 9325.
22. Siripitayananon, J.; Wangsoub, S.; Olley, R. H.; Mitchell, G. R. *Macromol. Rapid Commun.* **2004**, *25*, 1365.
23. Lipp, J.; Shuster, M.; Terry, A. E.; Cohen, Y. *Langmuir* **2006**, *22*, 6398.
24. Nogales, A.; Olley, R. H.; Mitchell, G. R. *Macromol. Rapid Commun.* **2003**, *24*, 496.
25. Nogales, A.; Mitchell, G. R. R.; Vaughan, A. S. *Macromolecules* **2003**, *36*, 4898.
26. Phillips, A. W.; Bhatia, A.; Zhu, P.-w.; Edward, G. *Macromol. Mater. Eng.* **2013**, *298*, 991.
27. Lai, W.-C.; Liao, J.-P. *Mater. Chem. Phys.* **2013**, *139*, 161.
28. Dong, M.; Guo, Z. X.; Yu, J.; Su, Z. Q. *J. Polym. Sci. Part B: Polym. Phys.* **2009**, *47*, 314.
29. Dong, M.; Guo, Z.; Yu, J.; Su, Z. *J. Polym. Sci. Part B: Polym. Phys.* **2008**, *46*, 1725.
30. Shepard, T. A.; Delsorbo, C. R.; Louth, R. M.; Walborn, J. L.; Norman, D. A.; Harvey, N. G.; Spontak, R. J. *J. Polym. Sci. Part B: Polym. Phys.* **1997**, *35*, 2617.
31. Lipp, J.; Shuster, M.; Feldman, G.; Cohen, Y. *Macromolecules* **2007**, *41*, 136.

32. Raab, M.; Šťudla, J.; Kolařík, J. *Eur. Polym. J.* **2004**, *40*, 1317.

33. Shi-Wei, W.; Wei, Y.; Ya-Jun, X.; Bang-Hu, X.; Ming-Bo, Y.; Xiang-Fang, P. *Polym. Test.* **2008**, *27*, 638.

34. Jones, A. T.; Aizlewood, J. M.; Beckett, D. R. *Die Makromol. Chem.* **1964**, *75*, 134.

35. Menyhard, A.; Varga, J.; Molnar, G. *J. Therm. Anal. Calorim.* **2006**, *83*, 625.

36. Dong, M.; Jia, M. Y.; Guo, Z. X.; Yu, J. A. *Chin. J. Polym. Sci.* **2011**, *29*, 308.

37. Balzano, L.; Rastogi, S.; Peters, G. *Macromolecules* **2011**, *44*, 2926.

38. Bai, H. W.; Wang, Y.; Song, B.; Li, Y. L.; Liu, L. *Polym. Eng. Sci.* **2008**, *48*, 1532.

39. Luo, F.; Wang, K.; Ning, N.; Geng, C.; Deng, H.; Chen, F.; Fu, Q.; Qian, Y.; Zheng, D. *Polym. Adv. Technol.* **2011**, *22*, 2044.

40. Phillips, A. W.; Bhatia, A.; Zhu, P.-w.; Edward, G. *Macromolecules* **2011**, *44*, 3517.

41. Shen, B.; Liang, Y.; Kornfield, J. A.; Han, C. C. *Macromolecules* **2013**, *46*, 1528.

42. Balzano, L.; Rastogi, S.; Peters, G. W. M. *Macromolecules* **2007**, *41*, 399.